

Impact of correlated magnetic noise on directional stochastic gravitational-wave background searches

Presented by **Stavros Venikoudis**

In collaboration with

Federico De Lillo, Kamiel Janssens, Jishnu Suresh and Giacomo Bruno

Centre for Cosmology, Particle Physics and Phenomenology (CP3),
Universite catholique de Louvain, Louvain-la-Neuve, B-1348, Belgium and
Universiteit Antwerpen, Prinsstraat 13, 2000 Antwerpen, Belgium



Sources of correlated magnetic noise

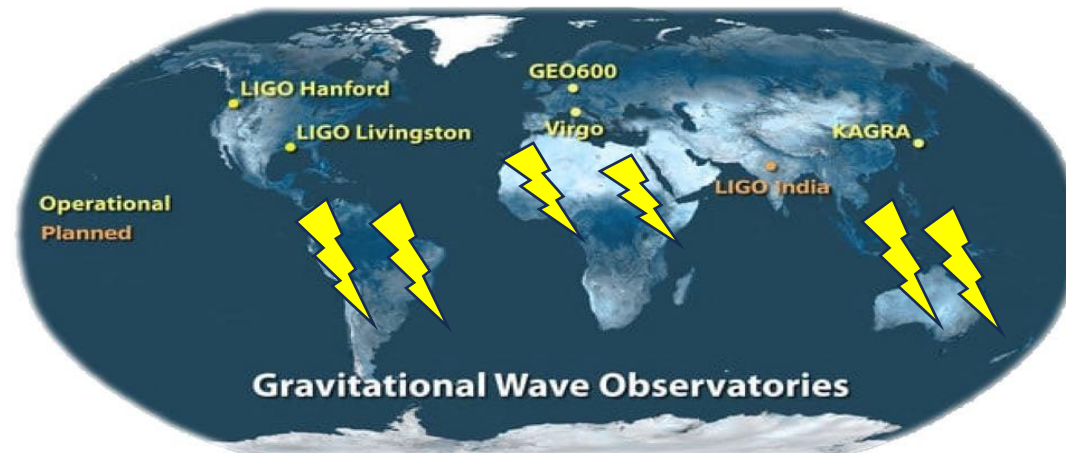
- Schumann resonances (8Hz – 60Hz)

Definition: Electromagnetic excitations formed inside the conducting cavity between the Earth and the ionosphere, generated by atmospheric dischargers.

Characteristic eigenmodes: 7.83Hz, 14.1Hz, 20.3 Hz

$$f_{\text{Schumann}} \simeq \frac{c\sqrt{l(l+1)}}{2\pi R_{\text{Earth}}} \quad \text{where } l = 1, 2, \dots$$

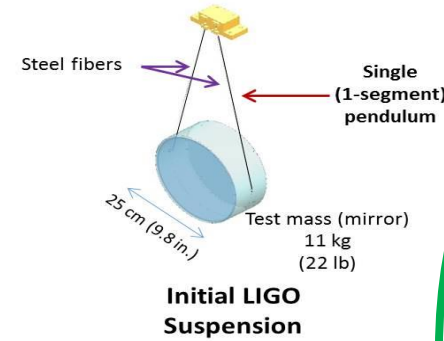
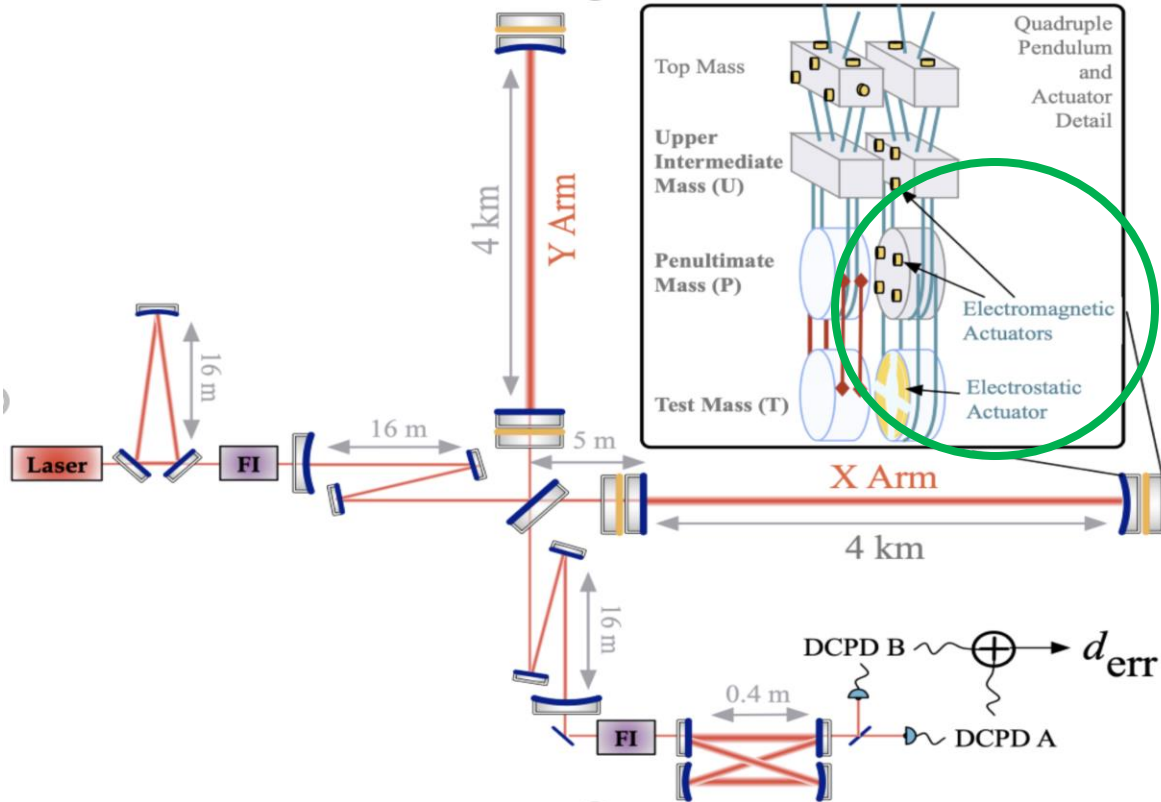
- Superposition of individual lightning strikes



Credits: map GW detectors-LIGO LAB/Virgo, available at ligo.org

Coupling of magnetic fields with GW-strain channels

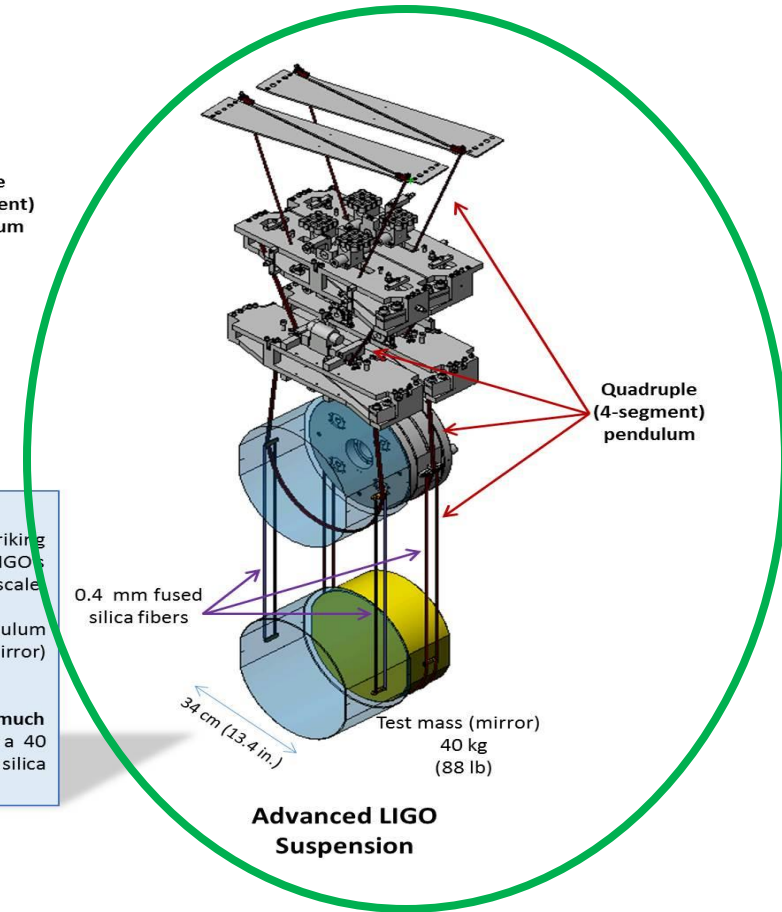
- Low frequencies: Coupling with permanent magnets of electromagnetic actuators and/or their suspensions



iLIGO vs aLIGO suspension systems
 These engineering drawings illustrate the striking differences between Initial- and Advanced LIGO suspensions. The suspensions are shown to scale.

Initial LIGO's suspension was a single pendulum design with an 11 kg (22 lb) 'test mass' (mirror) hung by steel fibers.

Advanced LIGO's suspension system is a much heavier quadruple ("quad") pendulum with a 40 kg (88 lb) 'test mass' (mirror) hung by fused silica fibers.



- High frequencies: Interaction with signal cables

Cross-Correlation statistic in the presence of correlated magnetic noise

- Output of detectors
$$\begin{aligned}\tilde{s}_I(f) &= \tilde{h}_I(f) + \tilde{n}_I^{\text{inst}}(f) + \tilde{n}_I^{\text{mag}}(f) \\ \tilde{s}_J(f) &= \tilde{h}_J(f) + \tilde{n}_J^{\text{inst}}(f) + \tilde{n}_J^{\text{mag}}(f)\end{aligned}$$

signal Detector noise Correlated magnetic noise

- Expectation value of cross-correlation

$$\langle \tilde{s}_I^*(f) \tilde{s}_J(f') \rangle = \langle \tilde{h}_I^*(f) \tilde{h}_J(f') \rangle + \langle \tilde{n}_I^{\text{inst}*}(f) \tilde{n}_J^{\text{inst}}(f') \rangle + \langle \tilde{n}_I^{\text{mag}*}(f) \tilde{n}_J^{\text{mag}}(f') \rangle$$

0

$$\langle \tilde{s}_I^*(f) \tilde{s}_J(f') \rangle = \langle \tilde{h}_I^*(f) \tilde{h}_J(f') \rangle + \langle \tilde{n}_I^{\text{mag}*}(f) \tilde{n}_J^{\text{mag}}(f') \rangle$$

- We measure the term $\langle \tilde{n}_I^{\text{mag}*}(f) \tilde{n}_J^{\text{mag}}(f') \rangle$

External magnetometers

- LEMI-120 at LIGO sites and Metronix MFS-06e at Virgo site (labelled i, j).
- Cross-correlation spectra of each magnetometer pair $I_i J_j$ for every GW detector baseline $\mathcal{I} = IJ = \{H, L, V\}$.

$$\tilde{m}_{\mathcal{I}}^{\text{mag}}(f) = \frac{2}{\tau} \left[|(\tilde{m}_{I_i}^* \tilde{m}_{J_i})(f)|^2 + |(\tilde{m}_{I_i}^* \tilde{m}_{J_j})(f)|^2 + |(\tilde{m}_{I_j}^* \tilde{m}_{J_i})(f)|^2 + |(\tilde{m}_{I_j}^* \tilde{m}_{J_j})(f)|^2 \right]^{1/2}$$

Magnetic coupling function (from the external magnetometers to GW-strain channel)



Outside to Inside (OTI)

Provides a level of shielding/amplification due to the building structure.

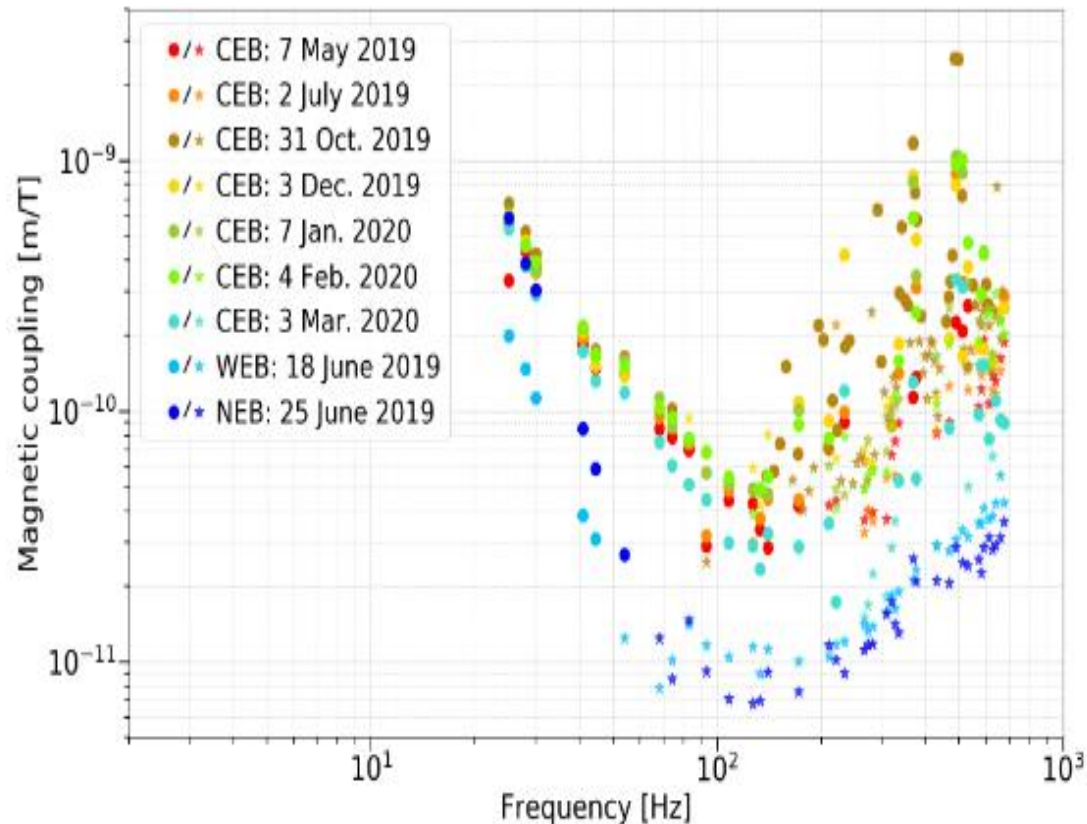


Inside to GW channel (ITC)

Encodes the key coupling features.

Inside to GW-channel coupling function

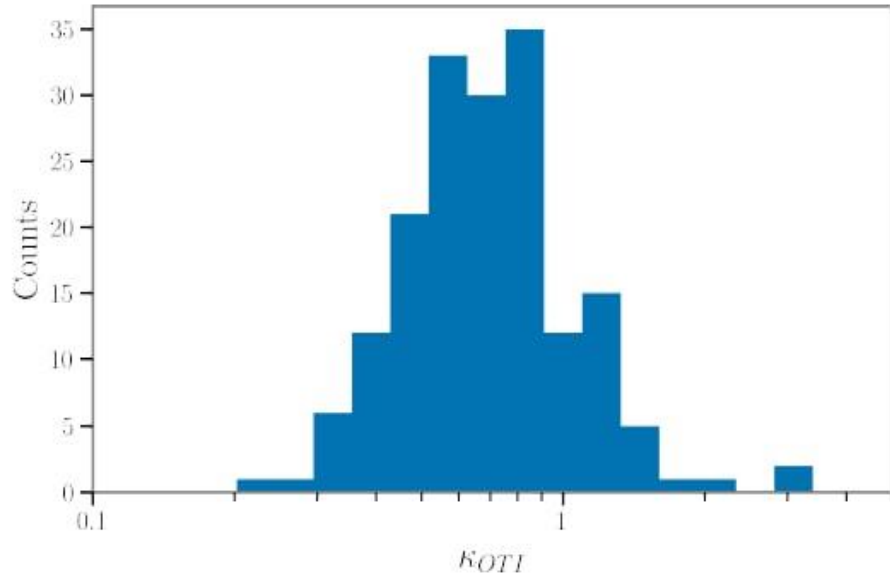
Measured through environmental noise injections inside the GW buildings.



Virgo

- LIGO: Measurements before and after O3 → max. value of every freq. bin
- Virgo: Weekly injection during O3 → average value

Outside-to-inside coupling function



Distribution of the outside-to-inside magnetic coupling based on 200 events.

Measurement of OTI:

Magnetic fields generated by lightning strikes near Livingston detector.

Log-normal distribution of coupling values with mean value 0.7 nT/nT.

Total magnetic coupling for every detector

$$\kappa_I(f) = \kappa_{I,OTI}(f) \cdot \kappa_{I,ITC}(f)$$

Directional searches for SGWB (1)

- Goal: Measure $\Omega_{\text{mag}}(f, \hat{\mathbf{n}}) = \frac{2\pi^2}{3H_0^2} f^3 \mathcal{P}_{\text{mag}}(f, \hat{\mathbf{n}})$ Angular power originating from the correlated magnetic noise term

- Decomposing the effective GW background angular power, induced by correlated magnetic noise in pixel basis,

$$\mathcal{P}_{\text{mag}}(f, \hat{\mathbf{n}}) = \sum_p \mathcal{P}_{\text{mag}_p}(f) e_p(\hat{\mathbf{n}}) \quad e_p(\hat{\mathbf{n}}) = \delta^2(\hat{\mathbf{n}} - \hat{\mathbf{n}}_p)$$

Pixel number

- The effective angular power spectra $\mathcal{P}_{\text{mag}}(f, \hat{\mathbf{n}})$ can be measured by using as statistic the maximum likelihood estimator.

$$\hat{\mathcal{P}}_{\text{mag}}(f) = \mathbf{\Gamma}_{\text{gw}}(f)^{-1} \mathbf{X}_{\text{mag}}(f)$$

Directional searches for SGWB (2)

- Dirty map $X_{\text{mag}_p}^{\mathcal{I}}(f) = \tau \Delta f \text{Re} \sum_t \frac{\gamma_{ft,p}^{\mathcal{I}*} \tilde{m}_{\mathcal{I}}^{\text{mag}}(f)}{\boxed{P_I(t; f) P_J(t; f)}} | \kappa_I(f) || \kappa_J(f) |$
Power spectral density

- Fisher matrix $\Gamma_{\text{gw}_{pp'}}^{IJ}(f) = \frac{\tau \Delta f}{2} \text{Re} \sum_t \frac{\gamma_{ft,p}^{IJ*} \gamma_{ft,p'}^{IJ}}{P_I(t; f) P_J(t; f)}$

- Overlap reduction function $\gamma_{ft,p}^{\mathcal{I}} = \sum \boxed{F_I^A(\hat{\mathbf{n}}, t) F_J^A(\hat{\mathbf{n}}, t)} e^{2\pi f \hat{\mathbf{n}} \cdot \Delta \mathbf{x}_{\mathcal{I}}(t)/c}$
(A) Antenna pattern functions
A={+,x}

Directional searches for SGWB (3)

Adding more baselines significantly enhances the search results as more blind spots due to the antenna pattern functions of detectors are covered.

$$X_{\text{mag}}^{\text{HLV}}(f, \hat{\mathbf{n}}) = \sum_{IJ} X_{\text{mag}}^{IJ}(f, \hat{\mathbf{n}}), \quad \Gamma^{\text{HLV}}(f, \hat{\mathbf{n}}) = \sum_{IJ} \Gamma_{\text{gw}}^{IJ}(f, \hat{\mathbf{n}}),$$

$$\hat{\mathcal{P}}_{\text{mag}}^{\text{HLV}}(f, \hat{\mathbf{n}}) = \Gamma^{\text{HLV}}(f, \hat{\mathbf{n}})^{-1} X_{\text{mag}}^{\text{HLV}}(f, \hat{\mathbf{n}}) \quad \sigma_{\hat{\mathbf{n}}}(f) = [\Gamma_{\hat{\mathbf{n}}, \hat{\mathbf{n}}}(f)]^{-1/2}$$

Sky pixelization

Tool: Hierarchical Equal Area isoLatitude Pixelization (HEALPix)

Parameter: $N_{\text{side}} = 8$ $N_{\text{pixel}} = 12N_{\text{side}}^2 = 768$

Results

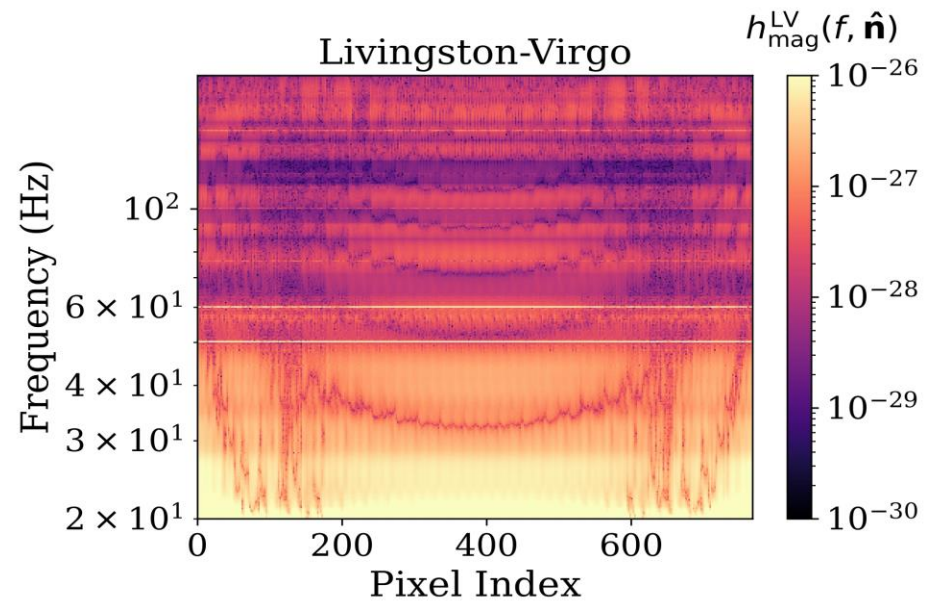
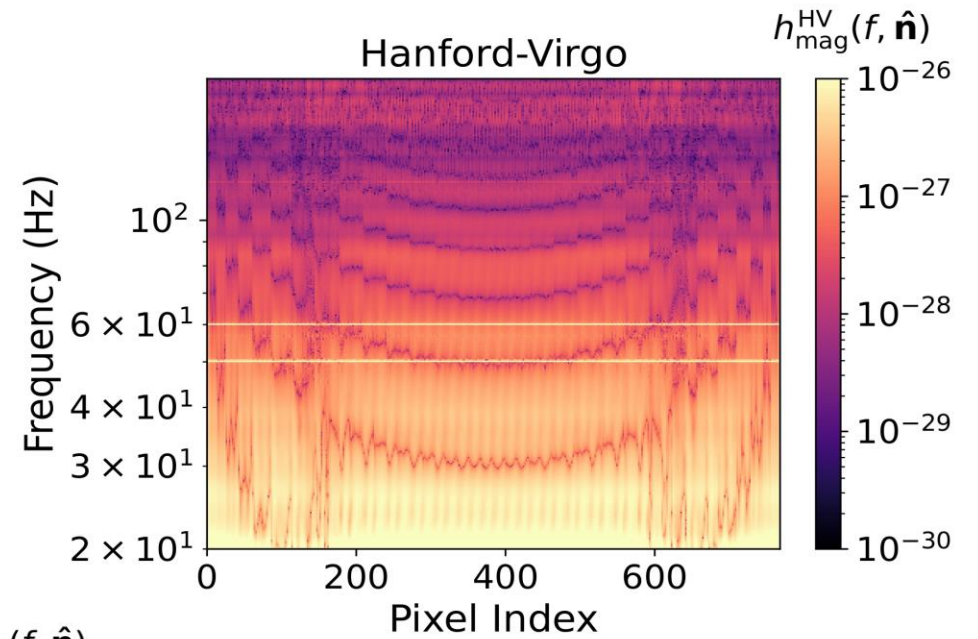
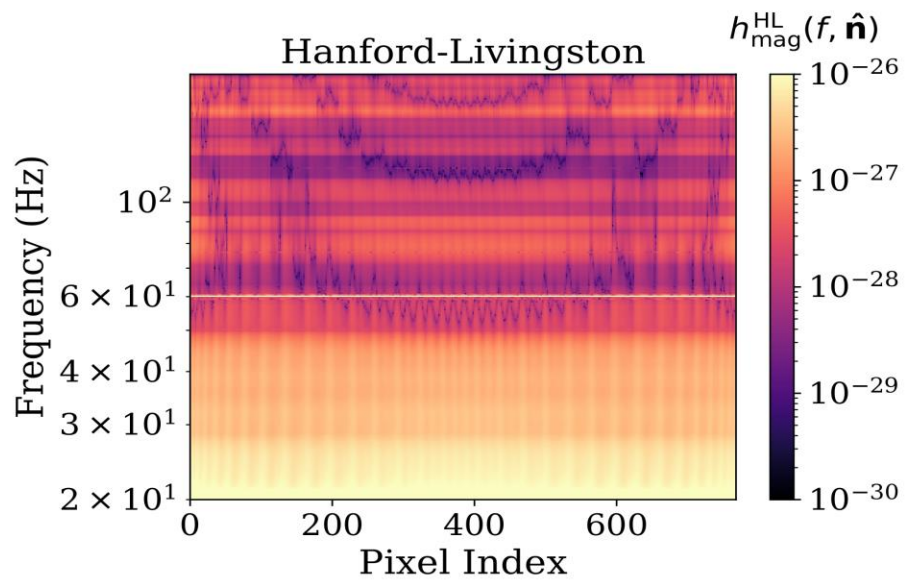
Estimation of the impact of correlated magnetic noise on:

1. All-sky, all-frequency (ASAF) directional searches
2. Broadband (BBR) searches
3. Isotropic searches

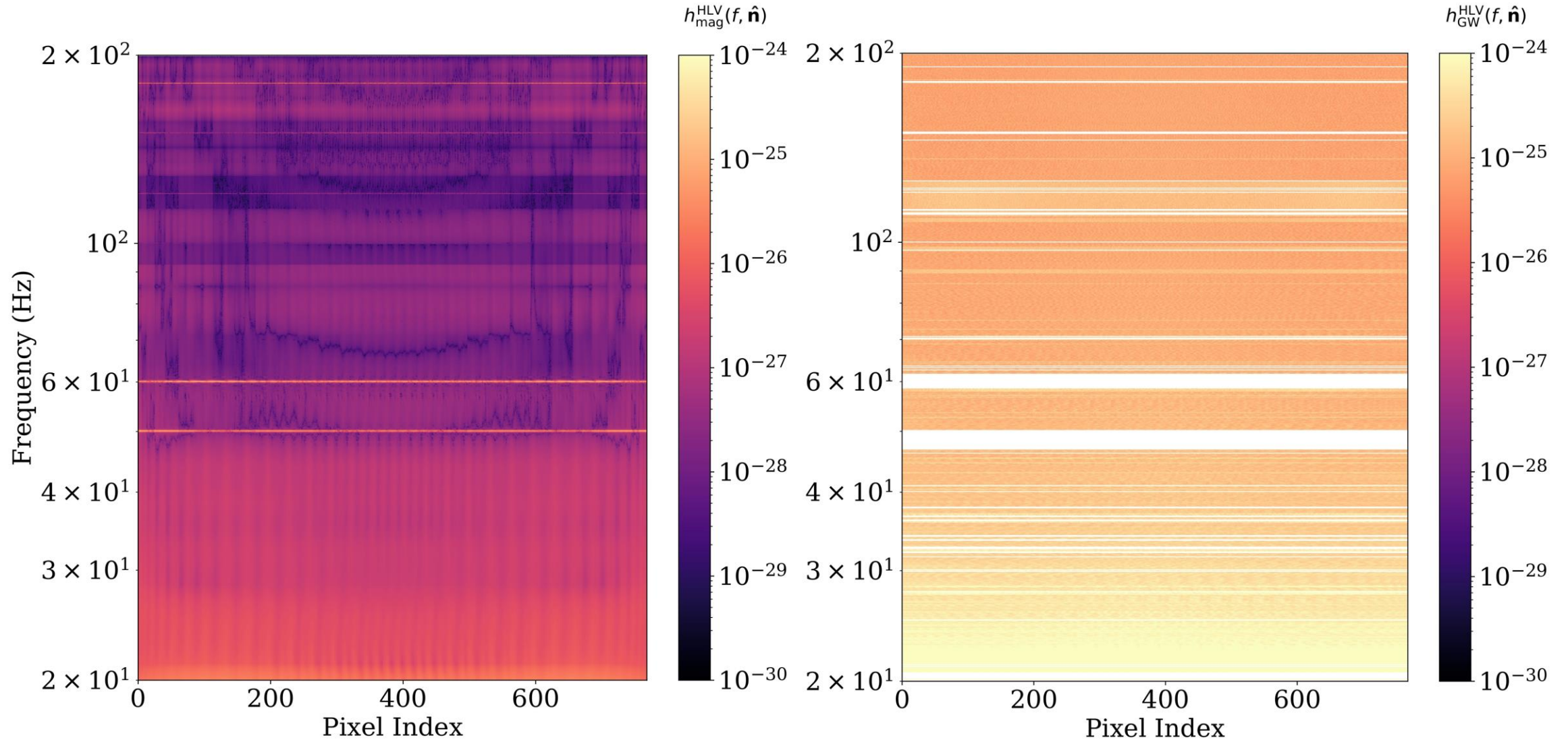
Impact on ASAF directional SGWB searches

- ASAF : Unmodeled search for unknown persistent signals in narrow frequency bins.
- Effective GW strain of magnetic origin $h_{\text{mag}}(f, \hat{\mathbf{n}}) = \sqrt{\mathcal{P}_{\text{mag}}(f, \hat{\mathbf{n}})\Delta f}$

Effective GW-strain induced by correlated magnetic noise



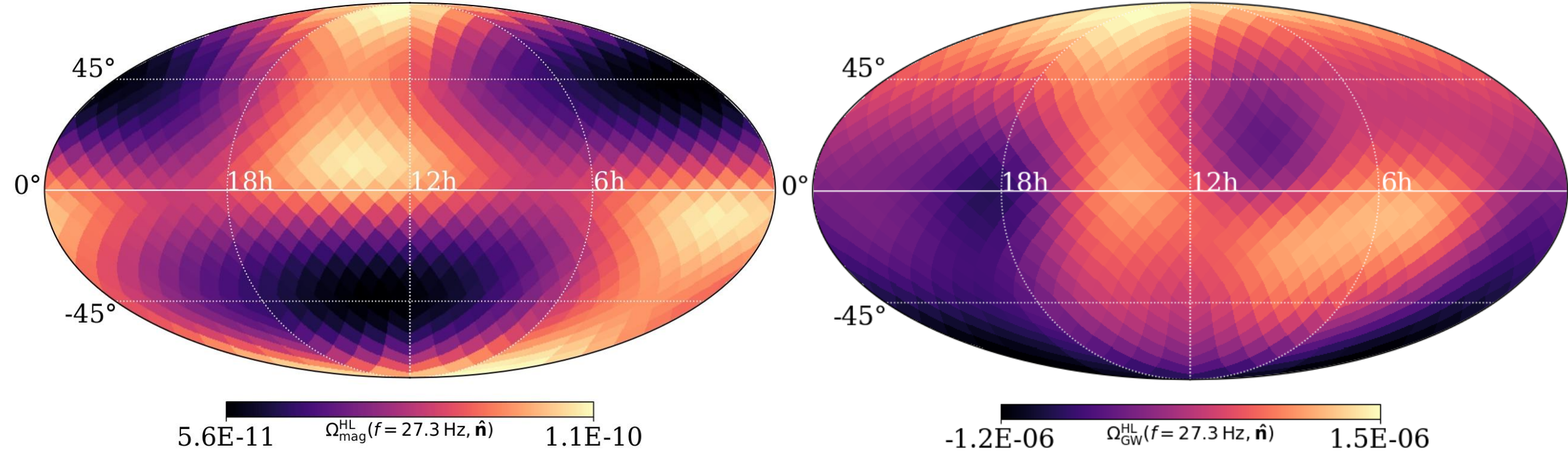
Impact on ASAF directional SGWB searches



Effective GW strain induced by magnetic correlated noise

95 % U.L. h_{gw} from O3 run

4th Schumann resonance peak of 27.3 Hz



Intensity of the effective GW energy density as Mollweide projection of the sky in equatorial coordinates at 27.3 Hz for HL baseline (left sky map) and GW energy density on the right.

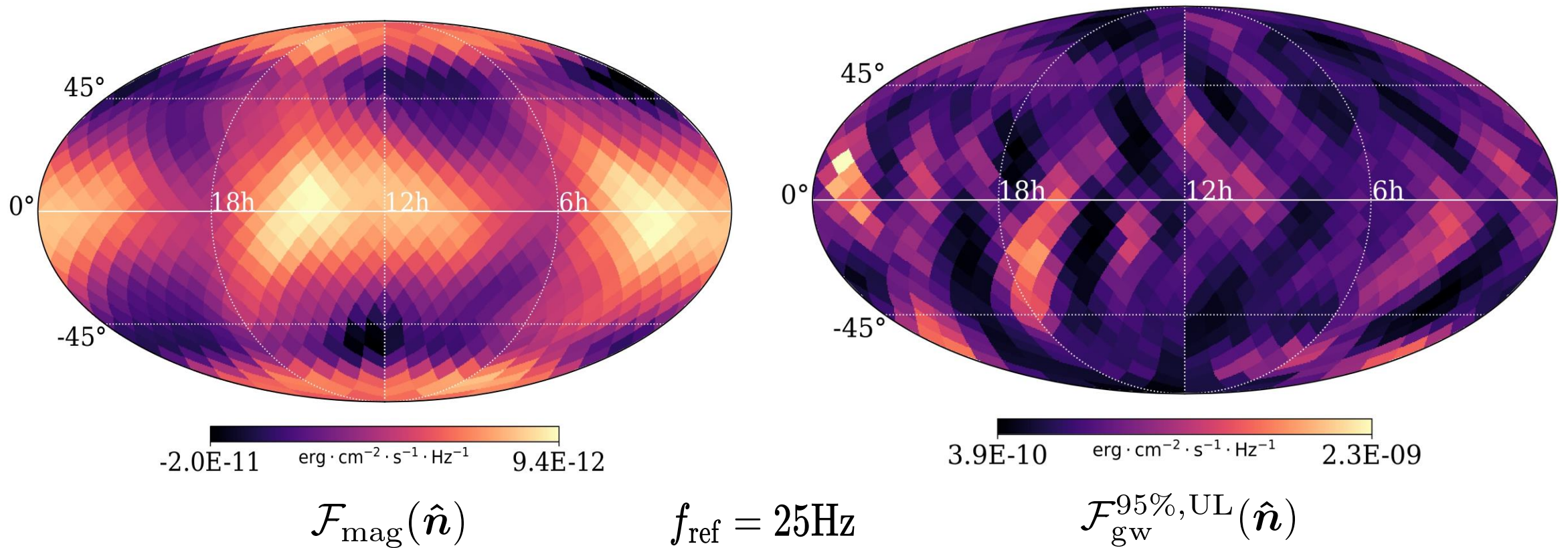
Impact on Broadband Radiometer searches

- Motivation: The broad-band radiometer (BBR) search is focused on sources that emit GWs over a wide frequency band.
- Schumann resonances have broad-band features (8 – 60 Hz)
- We apply a discrete integration to the effective anisotropic estimator over the entire frequency range 20-200Hz.

$$\hat{\mathcal{P}}_{\text{mag}}(f_{\text{ref}}, \hat{\mathbf{n}}) = \frac{\sum_f \hat{\mathcal{P}}_{\text{mag}}(f, \hat{\mathbf{n}}) \sigma_{\hat{\mathbf{n}}}^{-2}(f) H_{\text{mag}}(f)}{\sum_f \sigma_{\hat{\mathbf{n}}}^{-2}(f) H_{\text{mag}}^2(f)} \quad H_{\text{mag}}(f) = \frac{\Omega_{\text{mag}}(f)}{\Omega_{\text{mag}}(f_{\text{ref}})} \left(\frac{f}{f_{\text{ref}}} \right)^{-3}$$

- Effective GW flux in every sky direction $\mathcal{F}_{\text{mag}}(\hat{\mathbf{n}}) = \frac{c^3 \pi}{4G} f_{\text{ref}}^2 \mathcal{P}_{\text{mag}}(\hat{\mathbf{n}})$

Impact on Broadband Radiometer searches



Comparison between the effective GW flux from correlated magnetic noise measurements (left sky map) with the broadband flux of strain (right sky map) for the LVK detector network. The right sky map of the GW flux corresponds to a flat power spectral density labelled with $\alpha=3$.

Impact on Isotropic SGWB-searches

- Isotropic effective GW estimator induced by correlated magnetic noise

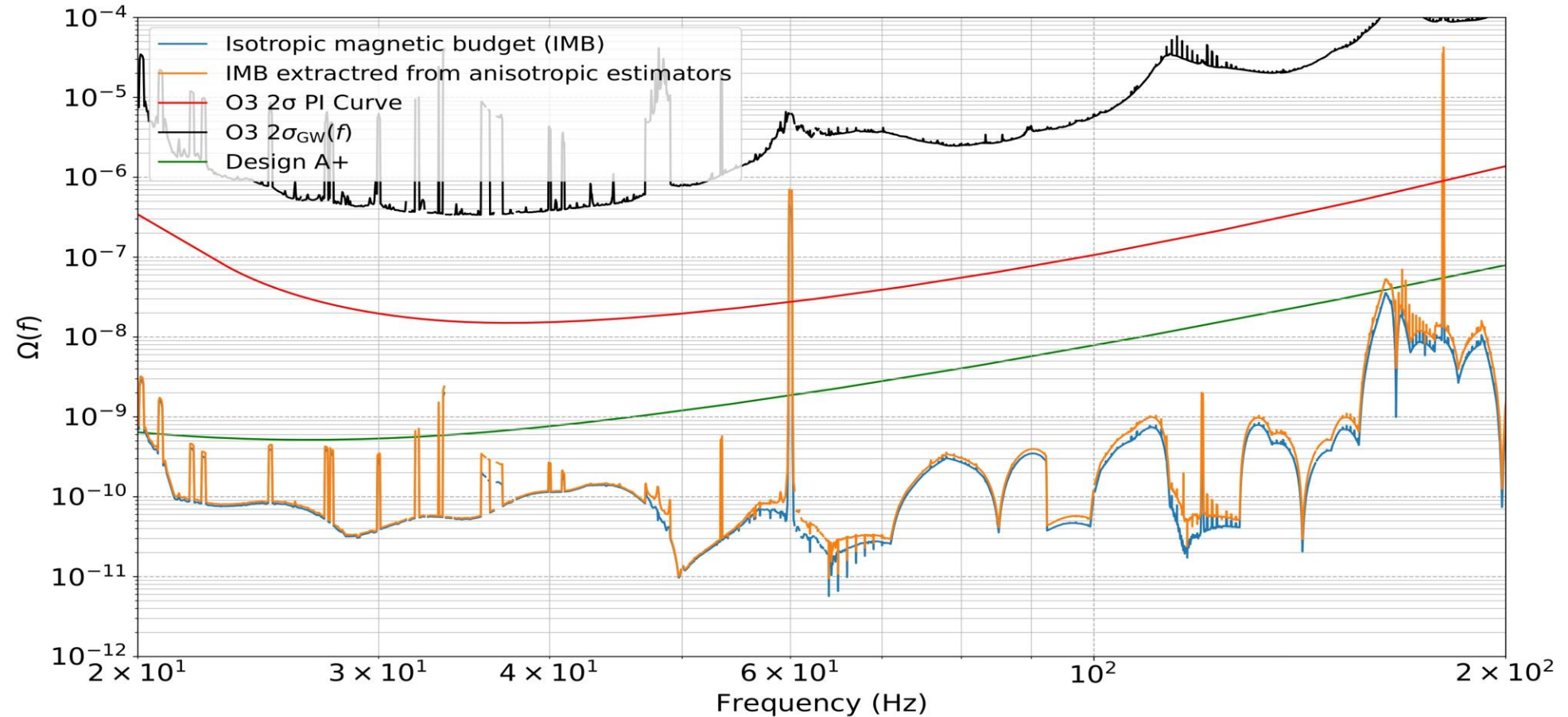
$$\hat{\mathcal{P}}_{\text{iso}} \sigma_{\text{iso}}^2(f) = \frac{5}{4\pi} \int d\hat{\mathbf{n}} \hat{\mathcal{P}}_{\text{mag}}(f, \hat{\mathbf{n}}) \sigma_{\hat{\mathbf{n}}}^{-2}(f)$$

$$\sigma_{\text{iso}}^{-2}(f) = \left(\frac{5}{4\pi}\right)^2 \int d\hat{\mathbf{n}} \int d\hat{\mathbf{n}}' \Gamma_{\hat{\mathbf{n}}, \hat{\mathbf{n}}'}(f)$$

↓
Full fisher matrix

$$d\hat{\mathbf{n}} = 4\pi/N_{\text{pix}}$$

Isotropic magnetic budget



Reference: Kamiel Janssens et al. Correlated 1–1000 Hz magnetic field fluctuations from lightning over Earth-scale distances and their impact on gravitational wave searches. Phys. Rev. D, 107(2):022004, 2023. doi:10.1103/PhysRevD.107.022004

Conclusions

- Correlated magnetic noise did not affect searches for isotropic and anisotropic SGWBs during the O3 LVK run.
- The possibility that Schumann resonances could limit the sensitivity of terrestrial detectors to SGWB in the frequency range of 20-30 Hz in the future runs, particularly after the upgrade to Advanced LIGO+ and Advanced Virgo+ , is under investigation.

Thank you for your attention!